Journal of Materials Processing Tech. 256 (2018) 239–246

Contents lists available at ScienceDirect

Journal of Materials Processing Tech.

journal homepage: www.elsevier.com/locate/jmatprotec

Modelling of residual stresses in a narrow-gap welding of ultra-thick curved steel mockup

Chuan Liu[a,*], Jiawei Yang[a], Yifeng Shi[a], Qiang Fu[b], Yong Zhao[a]

[a] Provincial Key Lab of Advanced Welding Technology, Jiangsu University of Science and Technology, Zhenjiang 212003, China
[b] Nuclear Power Institute of China, Chengdu 610041, China

ARTICLE INFO

Keywords:
Residual stress
Narrow-gap welding
Ultra-thick mockup
Finite element method
Lumped-pass model

ABSTRACT

A plane strain model, an axisymmetric model and a lumped-pass three-dimensional (3D) model were employed to simulate the residual stresses in a narrow-gap welding 300 mm-thick curved steel mockup. The lumped-pass 3D model was built with the lumping scheme based on the two-dimensional (2D) temperature field result. The residual stresses on the top surface of the mockup were measured using the hole-drilling method and compared with the simulated stresses. Results show that the plane strain model cannot capture the asymmetric conditions of the curved mockup; the through-thickness transverse stress within the weld zone presents a self-equilibrated distribution, and the through-thickness hoop stress within the weld zone are almost tensile with the peak value occurring at a certain depth (8 mm) beneath the top and bottom surfaces.

1. Introduction

Welded structures contain significant levels of residual stresses, which have remarkable detrimental effects on the service performance and would lead to the abrupt and fatigue-related failure (Withers, 2007). Their adverse effect would be even worse for the large-scale, heavy-section welded structures due to the completely different distributions of residual stresses inside the structures from accumulated heat input.

Experiments have been adopted to evaluate the residual stress distribution inside heavy-section welded structures. For example, Smith and Garwood (1992) evaluated the effects of postweld heat treatment on residual stress levels in a 50 mm thick ferritic steel submerged-arc weld using the hole-drilling method and the block removal and layering method. Woo et al. (2011) used the neutron diffraction (ND) method to measure stress distribution through the thickness of a 50 mm thick welded joint produced by the electrogas welding technique, and they also measured the residual stress in welds with 70 mm and 80 mm thickness by the ND method, contour method and deep-hole method (Woo et al., 2013, 2015). Park et al. (2014) investigated the residual stress distribution in the 70 mm thick welds with the inherent strain method and ND method. Smith et al. (2000) adopted the deep-hole drilling method to measure the stresses in thick-section welds and components with the thickness in the range of 35 mm–108 mm.

Experimental methods cannot get the entire stress distribution within thick welded components. The finite element method (FEM), integrating with experiments, is usually used to investigate the full residual stress distribution in thick components. Since the computation cost for the thick-section components would be unaffordable, especially for a three-dimensional (3D) model, two-dimensional (2D) models are employed for most simulations on heavy-section components. For example, Liu et al. (2011) adopted the hole-drilling method to measure the surface stress in two 75 mm- thick 304L austenitic steel girth welds with an outer diameter of 680 mm and a length of 320 mm, axisymmetric finite element models were used to investigate the stress distribution and its evolution during welding. Jiang et al. (2017) studied the through-thickness distributions of the welding residual stress in the range of 50 mm–100 mm thick plates by using 2D models and the ND measurement, and they found both the heat input and plate thickness have little influence on the residual stress distribution due to the relatively large constraints of the thick specimen applied to each welding pass. Lindgren et al. (1999) adopted a 2D model to simulate the welding residual stress in a 200 mm thick welded plate and the simulated results were compared with the experimental ones by the hole-drilling method. Tan et al. (2014) used a lumped-pass model to investigate the welding residual stress in a 150 mm thick nuclear rotor steel pipe based on an axisymmetric model and the simulated results were verified by the experimental data with the local removal blind-hole method. Mitra et al. (2016) employed a plane strain model to simulate the residual stress distributions in 800 mm thick joints produced by the narrow gap submerged arc welding, and the simulated results were verified with the X-ray diffraction (XRD) measurement.

---

* Corresponding author.
E-mail addresses: mse.chuanliu@gmail.com, chuanliu@just.edu.cn (C. Liu).

https://doi.org/10.1016/j.jmatprotec.2018.02.024
Received 20 August 2017; Received in revised form 14 February 2018; Accepted 16 February 2018

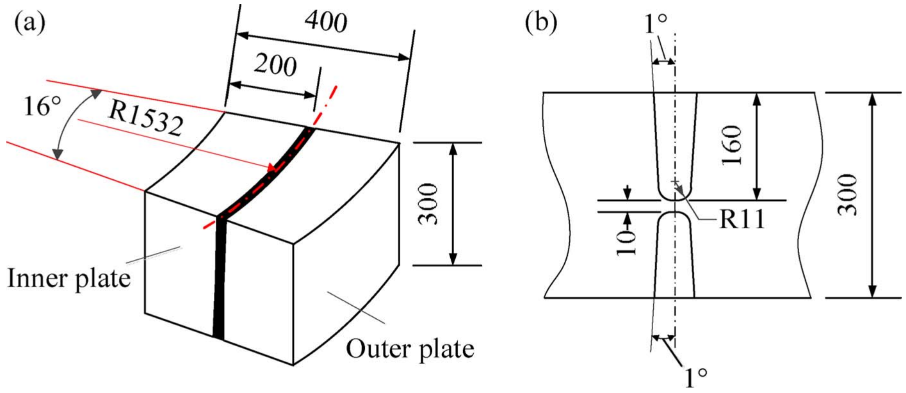

Fig. 1. Schematic diagram of the mockup: (a) Dimensions and (b) groove configuration.

Most researches focused on the residual stress in thick specimens with the thickness less than 100 mm and the 2D finite element model were the most popular numerical model in consideration of computation cost. The complex component cannot be simulated by 2D models because only a plane of the weld is considered, efficient 3D models with simplifications and enough simulation accuracy must be developed to model the welding residual stress in complex thick components. In the present study, the residual stress in a 300 mm thick curved specimen was investigated based on experiment and the finite element method. A mockup was manufactured with the multi-pass narrow gap welding and an efficient lumped-pass 3D model was developed based on the 2D temperature field result to simulate the full welding residual stress distribution. The simulated stresses were compared with experimental results.

2. Experimental procedure

The mockup consisted of two curved plates, which were butt-welded together with the narrow gap submerged arc welding. The dimensions of the mockup and the groove configuration are shown in Fig. 1. One curved plate is a section of a ring with a relatively small diameter and it is named inner plate, another is a section of a relatively large ring and is named outer plate, as shown in Fig. 1. The base metal 16MND5 (French vessel steel, equivalent to ASTM A533B Class 2 and ASTM SA508 Class 3) is a low-alloy steel mainly used as structural material in nuclear power plants. The mockup was built to investigate the welding residual stress of a ring welded to a cylinder, which is the common welded structure in the nuclear reactor pressure vessel. The chemical compositions of the base metal and the weld metal are shown in Table 1. An automatic rotation worktable was used to perform the welding.

There are three steps to complete the welding, as shown in Fig. 2. The top part of the groove was first filled to a height of 120 mm with 51 passes, and then the bottom part of the groove was filled with 61 passes after the root passes were removed by the carbon arc gouging, then the remaining height of the top groove was filled with 16 passes. Four restraining plates were welded to the worktable and the mockup to restrain the mockup during the first welding step, and the restraining plates were removed during the remaining welding procedure. The preheating temperature ranges from 225 °C to 275 °C and the interlayer temperature is kept in a range of 175 °C–250 °C. The welding parameters used are shown in Table 2. The photo of the mockup is shown in Fig. 3.

The hole-drilling method (ASTM International, 2008) was used to measure the residual stress on the top surface. A strain rosette (type A) was adhered to the surface and a hole with a diameter of 1.5 mm and a depth of 2 mm was drilled at the center of the strain rosette, and a strain recorder was used to record the strains due to the stress release, the stress at the measured point can be calculated according to the recorded strains. Because a stainless weld overlay cladding will be applied on the bottom surface of the mockup to investigate the effect of cladding on the welding stress (the investigated results will be processed later), only the stress on the top surface of the mockup was measured.

According to the ASTM standard E837 (ASTM International, 2008), it is possible to evaluate the stresses with only one set of the strain measurements (ε_1, ε_2, and ε_3), for example, the values at the maximum hole depth. Such a calculation could be useful to give a quick residual stress estimate. The hole was continuously drilled to the maximum depth in the present study, the longitudinal stress σ_x (along the welding direction) and the transverse stress σ_y (along the direction perpendicular to the weld) can be calculated using the measured strains at the maximun hole depth by the following equations:

$$\sigma_x = \frac{-E(\varepsilon_3 + \varepsilon_1)/2}{\bar{a}(1+\nu)} + \frac{E(\varepsilon_3 - \varepsilon_1)/2}{\bar{b}} \tag{1}$$

$$\sigma_y = \frac{-E(\varepsilon_3 + \varepsilon_1)/2}{\bar{a}(1+\nu)} - \frac{E(\varepsilon_3 - \varepsilon_1)/2}{\bar{b}} \tag{2}$$

Where, E is the elastic modulus, ν is the Poisson's ratio, $\bar{a}$ and $\bar{b}$ are the coefficients provided by the ASTM E837 standard. In the present study, the values of $\bar{a}$ and $\bar{b}$ are 0.111 and 0.297, respectively.

Additional strains can be induced by the hole-drilling procedure used in the present study and they have effects on the final measured stresses. According to Chen et al. (1994), the additional strain can be calculated by the following equation:

$$\varepsilon_{pm} = 0.194\varepsilon - 12 \tag{3}$$

Where, ε_{pm} is the additional strain induced by the hole-drilling procedure, ε is the measured strain after hole-drilling.

The values that the measured strains substracts the additonal strains are the final strains to calculate the measured stress.

Table 1
Chemical composition of base metal and weld metal/wt.%.

	C	Mn	Si	S	P	Mo	Cu	Fe
Base metal	≤ 0.22	1.15–1.60	0.1–0.3	≤0.012	≤0.02	0.43–0.57	≤0.02	Bal.
Weld metal	0.11	1.7	0.14	0.004	0.006	0.47	–	Bal.